JOURNAL OF APPLIED ENTOMOLOGY

J. Appl. Entomol.

ORIGINAL CONTRIBUTION

Temperature-dependent phenology and growth potential of the Andean potato tuber moth, *Symmetrischema tangolias* (Gyen) (Lep., Gelechiidae)

M. Sporleder[1], B. Schaub[2], G. Aldana[3] & J. Kroschel[1]

1 International Potato Center (CIP), Lima, Peru
2 Institute of Plant Production and Agroecology in the Tropics and Subtropics (380), Faculty of Agricultural Sciences, University of Hohenheim, Stuttgart, Germany
3 Agroklinge SA, Ate, Lima, Peru

Keywords
development rate models, life table statistics, modelling, *Phthorimaea operculella*, potato pests, potato tuber moth, temperature-dependent development

Correspondence
Marc Sporleder (corresponding author), International Potato Center (CIP), Lange Straße 59, 37 139 Adelebsen, Germany.
E-mail: marcsporleder96@gmail.com

Received: August 20, 2015; accepted: February 25, 2016.

doi: 10.1111/jen.12321

Abstract

The Andean potato tuber moth, *Symmetrischema tangolias* (Gyen) [Lepidoptera, Gelechiidae], is an economically important pest of potato (*Solanum tuberosum* L.) in the mid-elevated Andean region and an invasive pest of partially global importance. Determination of the pest's population life table parameters is essential for understanding population development and growth under a variety of climates and as part of a pest risk analysis. The development, mortality and reproduction were studied in two pest populations (from Peru and Ecuador) in which cohorts of each life stage were exposed to different constant temperatures ranging from 10°C to 28°C. Using the Insect Life Cycle Modeling software, nonlinear equations were fitted to the data and an overall phenology model established to simulate life table parameters based on temperature. The temperature-dependent development curve was statistically well described for eggs by Ratkowsky's model and for larvae and pupae by Taylor's model. Variability in development time among individuals independent of temperature was significantly described by a log-logistic model. Temperature effects on immature mortality were described using different nonlinear models. Optimal temperature for survival was between 14° and 17°C. Temperature effects on adult senescence and oviposition time were described by simple exponential models; within-group variability was described by a Weibull distribution function. Fecundity per female due to temperature followed a nonlinear model indicating maximum reproduction at ~17°C. The established model revealed good convergence with historical life tables established at fluctuating temperatures. The results confirm that *S. tangolias* is more adapted to cooler temperature than the common potato tuber moth, *Phthorimaea operculella* (Zeller). *S. tangolias* develops at temperatures within the range of 8–28.8°C with a maximum finite rate of population increase (=1.053) at 21°C. The established process-based physiological model can be used globally to simulate life table parameters for *S. tangolias* based on temperature and should prove helpful for evaluating the potential establishment risk and in adjusting pest management programmes.

Introduction

The Andean potato tuber moth, *Symmetrischema tangolias* (Gyen) [Lepidoptera, Gelechiidae], is likely native to the mountainous region of Peru and Bolivia. It causes significant economic damage to farmers growing potato (*Solanum tuberosum* L.) in the mid-elevated Andean region of South America (Palacios et al. 1999; Dangles et al. 2008) and is reported as a pest in New Zealand, Australia and the United States (Osmelak 1987; Martin 1999). In the Andes, the pest has expanded its range northwards from its assumed origin during the last several decades and today is established in some areas in Ecuador and Colombia. More recently, the pest was also recorded in Indonesia and Chile. Therefore, *S. tangolias* can be considered an invasive pest of partially worldwide proportion, although it has not spread as far as the common potato tuber moth, *Phthorimaea operculella* (Zeller), which currently has been reported in more than 90 countries worldwide (Kroschel et al. 2013). In South America and the Australian region, *S. tangolias* is known as a pest of potato and tomato (*S. lycopersicum* L.); however, in North America, it does not attack these crops but feeds on black nightshade (*S. nigrum* L.) and poroporo (*S. aviculare* G. Forst and *S. laciniatum* G. Forst) (Kroschel and Schaub 2013).

In the Andean region, *S. tangolias* is amalgamated with two other species of the family Gelechiidae: the common potato tuber moth and the Guatemalan potato tuber moth, *Tecia solanivora* (Povolny), referred to as the potato tuber moth complex. In particular in Peru, Bolivia and in some areas in Ecuador and Colombia, *S. tangolias* has become an economically significant species of the complex, like *P. operculella*, that attacks potatoes in both field and store. Although the three species are often considered sympatric in the region, they differ in many aspects of biology and damage (Kroschel and Schaub 2013). Compared with *P. operculella* and *T. solanivora*, there is evidence that *S. tangolias* is more adapted to cooler temperature conditions (Dangles et al. 2008). It prevails in mid-elevated regions of the Andes – typically above 2800–3000 m asl – but is not a pest at low altitudes, where *P. operculella*, which is the most widespread species of the complex, develops several generations per year (Keller 2003). The species of the complex may coexist in zones where temperature conditions are within the thermal limits of each species; however, the three species differ in their performance–temperature peak and in their feeding performance at their individual upper and lower thermal limits (Dangles et al. 2012). Recent studies showed that coexistence of potato tuber moth species results in higher crop damage than predicted from the effects of each species alone (Dangles et al. 2009, 2013). This increasing crop damage with greater richness of potato tuber moth species was explained by better resource utilization (feeding complementarities) and negative interactions, where intraspecific interactions are greater than interspecific ones. Keller (2003) found that although *P. operculella* was the dominant species infesting plants and tubers under field conditions in the Mantaro valley in Peru at altitudes of 3250–3500 m, *S. tangolias* was the more prevalent species under storage conditions, indicating clear habitat preferences of the two species. Recent monitoring studies of the flight activity of *S. tangolias* and *P. operculella* in the same valley confirm that *S. tangolias* is more active at altitudes of 3500–3800 m asl (J. Kroschel, unpublished).

It is well proven that temperature is one of the most important factors affecting development in ectothermic organisms (Uvarov 1931; Andrewartha and Birch 1954), and most of the models that describe insect development are based on temperature (Wagner et al. 1984; Logan 1988). The influence is explained by temperature's direct effects on enzymatic activities in insects (Schoolfield et al. 1981). In addition, temperature is a key abiotic factor influencing survival and reproduction rates in insects (Bale et al. 2002) and hence strongly determines the pest's demographic parameters, which are essential for interpreting population dynamics, developmental rates and seasonal occurrence (Campbell et al. 1974; Logan et al. 1976; McCornack et al. 2004). Detailed knowledge on temperature effects on herbivore insect pests can be used to determine the range where the pest might develop (establish) and to predict the population's growth potential (i.e. intrinsic rate of increase) and dynamics. In fact, each pest management programme requires an exact determination of the pest's population parameters (Zamani et al. 2006).

Although the biology and ecology of *P. operculella*, which is by far the most widespread species of the pest complex, have been extensively studied (reviewed by Kroschel and Schaub 2013), and temperature-driven phenology models have been established for *P. operculella* (Sporleder et al. 2004) and *T. solanivora* (B. Schaub, P. Carhuapoma, J. Kroschel forthcoming), substantial knowledge gaps on temperature effects exist for *S. tangolias* (Keller 2003). Dangles et al. (2009, 2012, 2013) thoroughly studied the ecology and interaction of the potato tuber moth species in the field and conducted life table studies on all three species at constant temperatures of 10°C, 15°C and 20°C (Dangles et al. 2008). The authors concluded

that *S. tangolias* is more adapted to lower temperatures and explained the species' distribution and impact in the Andean region by altitude. Despite the current knowledge on the species, the pest's capacity to disperse to new ecological zones cannot be predicted because the effect of temperature on life-history parameters is not known for the whole temperature range where *S. tangolias* might develop.

The objective of this study was to determine the nonlinear relationship between temperature and *S. tangolias* development, survival and fecundity, through constant temperature experiments. Second, we aimed to establish an overall temperature-driven phenology model for the pest, providing means of predicting potential increase of field populations with their seasonal variation in different ecologies around the world. We validated the model using historical life table data obtained at fluctuating temperatures from Keller (2003). This study is part of the effort to establish phenology models for major insect pests of potato and map the establishment risk and performance capacity of these pests in potato production regions worldwide (J. Kroschel, N. Mujica, P. Carhuapoma, M. Sporleder, forthcoming).

Materials and Methods

Origin and maintenance of *S. tangolias* colonies

Moths used in this study were derived from two laboratory colonies of *S. tangolias*. One was maintained at the International Potato Center (CIP), Lima, Peru, which started with moths collected from potato stores in Huancayo, Peru (3300 m asl). The second was maintained at the National Institute for Agricultural Research ('Instituto Nacional Autónomo de Investigaciones Agropecuarias' or INIAP, Santa Catalina Experimental Station, Quito), which started with moths collected from Santa Catalina, Ecuador (3050 m asl). Reared moths have been maintained on potato tubers at 20°C and >60% relative humidity and a photoperiod of 12 : 12 h light (L): dark (D). Eggs were placed in breeding cups (30 × 20 × 7.5 cm) containing potato tuber as food and pieces of corrugated carton (cardboard) as a pupation site. Collected pupae were disinfected in a 0.3% sodium hypochlorite solution and placed in oviposition cups that were covered with cheesecloth. A filter paper on the cheesecloth provided an oviposition site after the emergence of adults. A 5% sugar solution on the top of the cheesecloth served as a food source. The filter paper was changed daily and the eggs employed for further rearing.

Data collection

Data collection in Peru and Ecuador followed the same protocol. The effect of temperature on the biology of *S. tangolias* was studied on cohorts of single life stages in controlled incubation chambers over a temperature range of 10–28°C (table 1). Temperatures in mid-elevated potato production zones in Ecuador and Peru >3000 m asl, where *S. tangolias* is principally distributed, rarely go below a mean monthly temperature of 10°C or above 25°C. Indoor data loggers (Hobo H8, Onset, MA) were placed inside the incubation cabinets to monitor temperature. Owing to changing availability of incubation chambers or moths, cohort replications as well as the number of moths per cohort were unbalanced. The experiment was completely randomized. In Peru, six constant temperatures were tested: 10, 15, 17, 20, 24 and 28°C (for eggs also at 13.2°C); in Ecuador, five temperatures were tested: 10, 15, 20.4, 25.4 and 27.8°C. Temperature fluctuation within the chambers did not exceed ±1°C. Relative humidity in the chambers was maintained >60% and the photoperiod regime was kept at 12 : 12 h (L : D).

Life stages were maintained and evaluated as follows:

Egg stage

Filter paper was placed on the oviposition cups at 7 : 00 PM and removed at 7 : 00 AM to ensure that all eggs of *S. tangolias* were laid during a 12-h time interval. Sections containing about 100 eggs each (eggs were counted with a binocular microscope, ×10 magnitude) were cut off, placed in Petri dishes (∅ 9 cm), sealed with parafilm and incubated at the required temperature. (The number of paper sections with eggs used per temperature and installation date varied depending on the amount of available eggs; see table 1 for exact numbers of individuals evaluated per temperature.) The number of hatched eggs was recorded daily. In total, 14 949 eggs were used. Data from cohorts incubated at the same time in the same chamber were pooled. The sample comprised 23 independent replications (batches).

Larval stage

A number of generally 50 neonate *S. tangolias* larvae (hatched at the same time within a 2-h interval) were transferred to 0.5-L plastic cups that contained two potato tubers (ca. 100 g of potato, in Peru: cv. 'Peruanita', in Ecuador: cv. 'Superchola') as food. The number of cups set up per installation date was unbalanced depending on the availability of neonate

Table 1 Median development times resulting from accelerated failure time modelling and observed survival rates in the immature *Symmetrischema tangolias* life stages at constant temperatures

		Eggs			Larvae			Pupae		
Temp. (°C)	Exp. Side	N[1] (no. of batches)	Median dev. time (days)[3]	Survival (%)	N (no. of batches)	Median dev. time (days)	Survival (%)	N (no. of batches)	Median dev. time (days)	Survival (%)
10	Ecuador	786 (2)	33.2 (32.9–33.4) a	77.6	800 (2)	108.6 (107.5–109.8) a	40.3	400 (1)	78.4 (77.7–79.2) a	67.8
10	Peru	2330 (3)	23.4 (23.3–23.6) b	82.1	923 (4)	94.6 (93.3–95.9) b	47.1	430 (1)	62.6 (61.8–63.4) b	72.6
13.2	Peru	855 (1)	14.7 (14.5–14.8) c	88.3						
15	Ecuador	781 (2)	14.4 (14.2–14.5) d	88.9	400 (1)	46.8 (46.2–47.5) d	68.3	400 (1)	25.3 (25.0–25.7) d	84.5
15.4	Peru	1319 (1)	13.8 (13.6–13.9) e	82.9	593 (2)	53.0 (52.3–53.7)c	71	319 (1)	35.9 (35.4–36.4) c	83.7
17	Peru	949 (3)	11.0 (10.9–11.1) f	87.2	800 (1)	36.5 (36.0–37.0) e	77.1	185 (1)	24.6 (24.2–25.0) d	87.6
20	Peru	2071 (3)	9.13 (9.05–9.21) g	83.4	1900 (4)	28.3 (28.0–28.7) f	71.8	609 (1)	19.1 (18.9–19.3)e	78.8
20.4	Ecuador	725 (2)	8.17 (8.09–8.25) h	90.8	673 (2)	29.1 (28.7–29.6) f	38.3	165 (1)	16.6 (16.3–17.0) f	57.6
24	Peru	2411 (2)	6.43 (6.37–6.49) i	71.5	900 (1)	23.0 (22.6–23.3) g	42.7	283 (2)	13.3 (13.1–13.5)g	75.3
24.4	Ecuador	708 (2)	5.45 (5.39–5.51) j	89.3	644 (2)	21.6 (21.2–22.1) h	24.4	140 (1)	11.2 (11.0–11.4) h	68.6
27.8	Ecuador	769 (1)	5.20 (5.14–5.26) j	74.5	678 (2)	22.1 (21.7–22.6) h	29.9	226 (1)	10.2 (10.0–10.4) i	38.5
28	Peru	1245 (1)	3.88 (3.83–3.92) k	62.5	450 (1)	19.8 (19.4–20.1) i	41.3	230 (1)	12.9 (12.5–13.2) g	60
Total survivors		14949 (23)			4621 (22)			2459 (12)		
ln(scale)[2]		*ln*(δ) =	−2.968 [0.0085]***			−2.925 [0.0124] ***			−3.035 [0.0174] ***	
Scale parameter		δ =	0.0514 (0.0509–0.0518)			0.0537 (0.0530–0.0543)			0.0481 (0.0472–0.0489)	

		Likelihood ratio test				Likelihood ratio test				Likelihood ratio test			
Model[4]	*ln* L	Δ*Deviance*	df	P	*ln* L	Δ*Deviance*	df	P	*ln* L	Δ*Deviance*	df	P
Intercept only	−39 580				−20 285				−10555			
λ: for each Temp.	−19 090	40 980	11	<0.001	−12 615	15 341	10	<0.001	−5583	9945	10	<0.001
λ: for each Batch	−17 906	2368	11	<0.001	−12 499	232	11	<0.001	−5580	6	1	0.016
λ and δ: for each B.	−15 995	3822	22	<0.001	−12 175	649	21	<0.001	−5340	479	11	<0.001
Saturated	−15 212	1566			−10 897	2554			−5107	466		

[1]N is the number of individuals evaluated at a given temperature; the number in parenthesis is the number of batches (replications in time).

[2]δ in the scale of the log-logistic link function used in the analysis because the link function revealed a lower AIC compared to the log-normal and Weibull link function; the figure in [] is the SE of *ln*(δ) followed by asterisks indicating the parameter value significance level (P < 0.05 = *, P < 0.01 = **, P < 0.001 = ***). The accumulated development frequency in relation to normalized age (time/median time) is calculated according to the log-logistic link function: accu. dev. freq. = $1-(1/(1+x^{\alpha}))$, where x is the normalized age (determined through rate summation), and $\alpha = 1/\delta$.

[3]Numbers in parenthesis are 95% confidence limits. Medians followed by different letters in the same columns are significantly different (P < 0.05) according to the AFT model.

[4]For each life stage, 4 models were fitted; λ and *ln*(δ) only (intercept only), λ_i for each temperature, λ_i for each batch (i.e. replication in time for each temperature), and λ_i and scale parameter *ln*(δ) for each batch. Each higher level model reduced the deviance significantly (see P-values); however, in all cases, the AICc revealed that models with a common scale parameter were more appropriate than the model with individual scales; therefore, a common scale across all temperatures can be expected.

larvae (at least four cups were set up at the same date per temperature). The cups were closed with a lid of which a part was replaced with fine muslin (0.1 μm) for ventilation. *S. tangolias* larvae normally leave tubers before pupation. A piece of corrugated carton was placed inside the container for providing pupation sites. Pupated individuals were recorded daily and removed from the container. In total, 8761 larvae were tested in 22 batches (replications in time).

Pupal stage

Newly developed pupae collected from a rearing box were individually transferred to transparent plastic tubes and incubated at the required temperature. The number of pupae incubated per temperature at the same time was uneven due to the variable numbers of newly developing pupae available in the insect rearing (see table 1). The number of emerging adults and their sex were recorded daily. The total sample comprised 3387 individuals and 12 batches.

In all stages, the numbers of individuals tested per temperature at the same time were unbalanced due to changing availability of test insects. Final numbers of test insects and batches per temperature are noted in table 1. For further details about the original data, see the supplement materials (Appendix S1).

Adult stage

Assessment of adult survival time and oviposition differed between experimental sites. In Peru, individual pupae collected from a rearing box were separated by sex. At the day of emergence, five females and five males were placed in a plastic cylinder (∅ 7 cm × 10 cm height) covered with muslin and incubated at the required temperature; at least five cylinders were incubated at the same time per temperature as replicates – n (♀) ≥ 25. Filter paper was placed on top of the muslin to provide an oviposition site. The inside of the plastic cylinder did not provide any favourable site for oviposition, and it was assumed that oviposition took place only on the filter paper. The filter paper was replaced daily at 8 : 00 AM and the number of eggs in the paper recorded. Adults were fed daily with 5% sugar solution dropped on the edge of the muslin. Survival time of individual adults was recorded by sex. In Ecuador, adult survival and oviposition were assessed individually from two different groups of adults. For the assessment of survival, emerging adults (n = 50 ♀ + 50 ♂) were placed individually in a cage (8 cm^3 plastic box) and dead individuals removed in daily intervals until all individuals of the cohort had died. The sex of removed adults was determined and recorded together with survival time of each individual. For the assessment of progeny, a second group of adults was caged (a number of four females with four males were caged together and replicated 4–6 times in each temperature) in plastic cylinders. The number of laid eggs was recorded as described above (see table 4 for the number of females used per temperature for the assessment of progeny).

Data for model validation

Historical data collected during 1998 and 2000 in Huancayo, Peru, by Keller (2003) were used to validate the model. Keller (2003) monitored development times and mortality in all immature *S. tangolias* life stages in cohort studies, from freshly laid eggs to adult emergence. Six cycles were compelled at natural temperature under protected (shaded) conditions (each cycle contained three cohort replications initialized with n = 100 insects each) over 18 months. Minimum and maximum daily temperatures were monitored using Hobos (Onset, MA) placed close to the test insects.

Data analysis and modelling

For data analysis and model development, the Insect Life Cycle Modeling (ILCYM) software package (Sporleder et al. 2013), version 4, was used. The package uses R-statistics (R Development Core Team, 2011) for all statistical calculations. Version 3 is currently available as an open source program downloadable at: https://research.cip.cgiar.org/confluence/display/ilcym/Downloads). Version 4 includes significant improvements in some statistical methods over version 3. As version 4 has not been fully completed and no further references on new tools are available, the statistical analysis and modelling methods employed in this work are fully described here.

Interval censored data (event occurred between two observation times) on development time of the different immature life stages, adult longevity and fecundity of females were submitted to survival analysis. Parametric accelerated failure time (AFT) models were adjusted to the data using the survreg procedure of the survival package in R-statistics. For development times, log-error distributions were assumed which is in line with Curry's (Curry et al. 1978) 'one-shape' theory. The shape parameter of the error distribution is assumed to be in relative relation to the median development time – in other words, normalized distributions are expected to have the same shape. The lognormal, log-logistic and Weibull model

was tested as distribution link function. For adult longevity and fecundity, in addition to the extreme value, logistic, Gaussian and exponential link functions were tested. For each model, the most appropriate distribution link function was chosen according to the maximum likelihood. The final model was then fitted at different levels of complexity; that is, data were grouped by (i) temperature (default model), (ii) insect batches (replications per temperature in time) and (iii) batches but an individual scale parameter was fitted to the data of each batch. These models were evaluated using a likelihood ratio test and by comparing Akaike's information criterion (AIC) (Akaike 1973). The latter is a well-known goodness-of-fit indicator when comparing two models for the same set of data and preferred over classical goodness-of-fit tests. The AIC value is AIC = $2k$–$2\ln(L)$, where k is the number of parameters in the model, and L is the maximized value of the model's likelihood function. In this study, the corrected AIC (AIC_c) (Hurvich and Tsai 1989) was used because it panelizes stronger extra parameters and reduces the probability of selecting overfitted models. The AIC_c value is $AIC_c = AIC + (2k \times (k + 1))/(n - k - 1)$, where n denotes the sample size. Models were compared by their relative likelihood (=$\exp[0.5 \times \Delta AIC_c]$, also called AIC's evidence ratio).

Median development, adult survival and reproduction times revealed for each insect batch using the best-fitting ATF model were submitted to nonlinear regression analysis (using the nls procedure; R-statistics) for evaluating the relationship between temperature and median time to event. Many different models were fitted to each type of data; for example, to median development times, >20 models that might describe temperature-dependent development in insects were tested. (See the list in the user manual ILCYM 3.0 [Tonnang et al. 2013], downloadable at: https://research.cip.cgiar.org/confluence/display/ilcym/Downloads, pp. 147–152.) Generally, these functions are fitted in term of rates (1/median time); however, in this study, the functions were fitted in terms of *ln* times to address increasing variances with increasing median development times (homogeneous variances across all groups are expected when median times are *ln*-transformed). Survivorship in immature life stages was calculated from the relative frequency of surviving test insects. Different nonlinear models (remodelled quadratic functions) were fitted by regression to describe the mortality rate in each life stage and fecundity by temperature. The modelled functions were based on the vertex form of the quadratic equation: $y = c(x–h)^2 + k$, with the intension to estimate the vertex (h, k) of the parabola; c is the shape parameter. The transformed models were able to describe both symmetric and asymmetric parabola. The most appropriate model for describing the temperature effect on any of the above parameters was chosen by comparing AIC_c as described above.

Life table parameters – namely net reproduction rate (R_0), mean generation time (T), intrinsic rate of natural increase (r_m), finite rate of increase (λ) and doubling time (Dt) – were calculated from the established models over a range of constant temperatures according to Maia et al. (2000) using the approximate method (approximate estimate for T). For model validation, Keller's temperature records (daily minimum and maximum temperature) were used as simulation input temperature. The simulation was conducted in 1-day intervals using a cohort updating algorithm, whereby for each day, a 15-min discrete time increment was used to account for within-day temperature fluctuations. The temperature at each time interval was predicted using a cosine-wave function between minimum and maximum temperature input data as described by Sporleder et al. (2013, p. 419). Each life table simulation was started with a number of 100 fresh eggs. Development to the next stage was calculated using the stage-specific temperature-dependent development rate function (table 2) in conjunction with the distribution shape parameter of the AFT model (table 1). That is, development rates were accumulated for each cohort and the proportion of individuals within the cohort developing to the next stage was calculated using the distribution function. For the log-logistic function, the accumulated development frequency in relation to the cohorts' physiological age is calculated using the formula:

$$\text{acc.dev.freq.} = 1 - \left(\frac{1}{[1 + \sum_{k=0}^{n} r(T)^{\alpha}]}\right)$$

where $\sum_{k=0}^{n} r(T)$ is the accumulated development rate over the period from stage initialization ($k = 0$) to the nth day depending on temperature, T, and $\alpha = 1/\delta$ is the stage-specific shape parameter of the curve, where δ is the scale parameter of the stage-specific distribution link function. The proportion of individuals that develop each day to the next stage forming a new cohort of the following stage is the accumulated development frequency of day x_i minus the accumulated development frequency of day x_{i-1}. Daily stage-specific survival rates were calculated using the formula:

Table 2 Models and their parameters fitted to describe temperature-dependent median development rates (1/day) in immature life stages of *S. tangolias*

Life stages	Model[2]	Parameters[1]		F-value	$df_{1,2}$	P	adj. R^2	Distribution scale parameter (α)
Egg	Root square	b	−0.0151 (±0.0007)***	534	1, 21	>0.001	0.9604	19.4
		Tb	−2.8397 (±0.8066)***					
Larvae	Taylor model	r_m	0.0476 (0.0017)***	2109	2, 19	>0.001	0.9901	18.6
		T_{opt}	28.58 (0.9)***					
		T_{roh}	10.5 (0.45)***					
Pupae	Taylor model	r_m	0.099 (±0.014)***	417	2, 9	>0.001	0.9742	20.8
		T_{opt}	31.8 (±3.2)***					
		T_{roh}	11.1 (±1.37)***					

[1]Numbers in parenthesis are standard errors. Parameter values significantly different from zero are indicated by asterisks (P < 0.05 = *, P < 0.01 = **, P < 0.001 = ***).
[2]Models: Root square: $r(T) = [b(T-\mathrm{Tb})]^2$ (Ratkowsky et al. 1982); Taylor model: $r(T) = r_m \exp[-0.5\{-(T-T_{opt})/T_\alpha\}^2]$ (Pradhan et al. 1945, Taylor 1981).
The distribution scale parameter for each life stage $\alpha = 1/\delta$ is drawn from table 1. The distribution link function is the log-logistic function. Hence, the accumulated development frequency in relation to the physiological age (determined through rate summation) is calculated using the formula:

$$acc.dev.freq. = 1 - \left(\frac{1}{[1 + \sum_{k=0}^{n} r(T)^{\alpha}}\right)$$

$$\text{survival} = (1 - m_i)^{r(T)}$$

where m_i is temperature-dependent mortality in stage i using the established mortality functions (table 3) and $r(T)$ is the stage-specific temperature-dependent development rate calculated as above (table 2). This formula assumes that the stage-specific daily survival rate, l_x, is temperature dependent but unique across all age classes (i.e. it assumes the exponential hazard rate function). Daily fecundity per female was calculated using the formula:

$$\text{daily fecundity per female} = (P_i - P_{i-1}) \times F(T)$$

where P_i is the accumulated proportion of eggs laid by a female depending on age. For the Weibull link function, P_i is calculated by:

$$P_i = 1 - \exp\left(-\exp\left(ln\left(\sum_{k=0}^{n} r(T) \times \exp(1)\right) \times \alpha\right) \times \exp(-\alpha)\right)$$

where $\sum_{k=0}^{n} r(T)$ is the accumulated median oviposition time^{-1} (see function in table 5) over the period from adult emergence to the nth day depending on temperature, T, and α is $1/\delta$, where δ is the scale parameter of the specific Weibull distribution link function (table 4); and $F(T)$ is the calculated total temperature-dependent fecundity per female using the established model (table 4). For model validation, Keller's temperature records (daily minimum and maximum temperature) were used as simulation input temperature. The developmental times and survival percentages resulting from these modelling were compared to the life table results observed by Keller (2003).

Results

Development time and its variation

The variation in development times among individuals across all temperatures (fixed variance) was best described in all three immature life stages using a log-logistic model (table 1). The model was fitted at different levels of complexity: first, estimating median development times for each temperature; second, estimating median development times for each batch of insects (replicates in time); and third, estimating median development times and an individual scale parameter for each batch. The likelihood ratio test revealed

Table 3 Models and their parameters fitted to describe temperature-dependent mortality in immature life stages of *S. tangolias*

Life stages	Model[1]	Parameters[2]		F-value	$df_{1,2}$	P	adj. R^2
Egg	$r(T) = \exp\,(ln[r_{min}] + c\{T_{opt} - T\}^2)$	T_{opt}	17.09 (±1.32)***	6.72	2, 20	0.006	0.1767
		r_{min}	0.131 (±0.023)***				
		c	0.007 (±0.0031)*				
Larvae	$r(T) = 1 - \frac{1}{\left(1+exp\left\{\frac{ln[r_{min}]+c\left[\frac{1}{\sqrt{T_{opt}}}-\frac{1}{\sqrt{T}}\right]^2}{}\right\}\right)}$	T_{opt}	14.6 (±0.35)***	30.3	2, 19	>0.001	0.5742
		r_{min}	0.38 (±0.084)***				
		c	383.3 (±78.6)***				
Pupae	$r(T) = \exp(ln[r_{min}]) + c\left\{\frac{1}{\sqrt{T_{opt}}} - \frac{1}{\sqrt{T}}\right\}^2$	T_{opt}	16.25 (±1.07)***	417	2, 9	0.002	0.4967
		r_{min}	0.185 (±0.038)***				
		c	0.617 (±0.232)*				

[1]The models used describe a parabola with its vertex at (T_{opt}, r_{min}); the parameter r_{min} is the lowest predicted mortality rate at the optimum temperature T_{opt}.
[2]Numbers in parenthesis are standard errors. Parameter values significantly different from zero are indicated by asterisks (P < 0.05 = *, P < 0.01 = **, P < 0.001 = ***).

that each increase in model complexity significantly improved the model in each life stage (table 1). For the egg and larval stages, however, the most appropriate model according to AIC_c values was the second model estimating median times for each batch with common scale parameters. This indicated that the individual scale parameters, δ_i, for each batch of test insects overfit the model; however, there was certain variation in median development times among the batches exposed to the same temperature (variable variance). The common scale parameters were highly significant (for each life stage P < 0.001) and adequate to describe the overall (fixed) variability in development times among individuals in each immature life stage.

Median development times showed a strong temperature dependency. The relationship between temperature and median developmental rates in eggs was among several statistically good-fitting models best described by Ratkowsky's root square model (which explained >96% of the variation in median development times by temperature), and in larvae and pupae by Taylor's model (explaining >99% and >97% of the variation, respectively) (fig. 1, table 2). Taylor's model predicted a development peak at temperatures above 28°C for larvae and pupae; thereafter, development decreased due to high temperature. The models were fitted in terms of *ln* time; therefore, the error estimated for prediction in terms of rates (as shown in fig. 1) increased with increasing development rates.

Immature mortality

The effect of temperature on the mortality of immature life stages was described by nonlinear functions (table 3, fig. 2). Mortality was quite variable in all stages. Optimum temperature for survival was around 14°C for larvae to 17°C for eggs. The model fitted to egg mortality explained only 17% of the variation by temperature, but the probability of the model and the three estimated parameters were significant (P < 0.05). Functions fitted between temperature and mortality in larvae and pupae (P < 0.05) showed skewing to low temperature (i.e. the mortality increased as temperature deviated from the optimum temperature, T_{opt}, but the increase was more pronounced at temperatures below the optimum temperature than at temperatures above the optimum). And the established models were adequate to describe temperature-dependent mortality within the temperature range tested, but the data are insufficient to reliably predict the minimum and maximum temperature thresholds for survival.

Table 4 Median survival times of *Symmetrischema tangolias* adults, median oviposition times and total fecundity per female at different constant temperatures

Temp. (°C)	Exp. Side	N[1] (no. of batches)	Median survival time (days)[3,4]		Median oviposition time[5] (days)	Mean fecundity/ female (eggs)
			Females	Males		
10	Peru	50/50 (1)	34.4 (±1.37)	32.2 (±1.81)	14.4 (±0.12)	85.2 (±8.3)
10	Ecuador	200/200 (1)	38.2 (±1.7)	35.8 (±1.6)	14.9 (±0.33)	45.9 (±0.7)
15	Peru	25/25 (1)	27.6 (±1.93)	24.9 (±1.75)	15.1 (±0.21)	102.5 (±4.8)
15	Ecuador	206/200 (1)	23.1 (±1.02)	25.3 (±1.13)	6 (±0.07)	236.7 (±6.7)
17	Peru	35/35 (2)	21.8 (±1.38)	20.6 (±1.3)	11.6 (±0.14)	111.2 (±54)
20	Peru	35/35 (2)	18.1 (±1.19)	17.6 (±1.15)	8.7 (±0.1)	133.6 (±27.8)
20.4	Ecuador	81/54 (1)	23.3 (±1.2)	22.5 (±1.26)	11 (±0.15)	187.8 (±46.5)
24	Peru	40/35 (1)	19.1 (±1.16)	17.6 (±1.11)	9.8 (±0.15)	44.9 (±17.7)
25.4	Ecuador	58/61 (2)	10.7 (±0.6)	8.9 (±0.49)	6.6 (±0.1)	94.7 (±42.8)
27.8	Ecuador	59/50 (2)	7.3 (±0.41)	6.5 (±0.38)	4.7 (±0.22)	9.9 (±3.9)
28	Peru	25/25 (1)	13.6 (±1)	12.3 (±0.89)	8.1 (±0.16)	39.8 (±18)
		814/770 (15)				
	λ_{sexm}		−0.0441 [0.013]***			
	$\ln(\delta)^2$ =		−1.456 [0.021]***		−0.596 [±0.005]***	
	δ =		0.244 (0.234–0.254)		0.551 (0.546–0.556)	

[1]N is the number of individuals evaluated at a given temperature (♀/♂); the number in parenthesis is the number of batches (replications in time).

[2]δ in the scale of the Weibull link function used in the analysis because the link function revealed a lower AIC compared to the log-normal and log-logistic link function; the figure in [] are the SEs of $ln(\delta)$ followed by asterisks indicating the parameter value significance level ($P < 0.05$ = *, $P < 0.01$ = **, $P < 0.001$ = ***). The accumulated development frequency in relation to normalized age (time/median time) is calculated according to the Weibull link function: accu. dev. freq. = $1-\exp\{-\exp(\ln[x \times \exp(1)] \times \alpha) \times \exp(-\alpha)\}$, where x is the normalized age (determined through rate summation, and $\alpha = 1/\delta$.

[3]Numbers in parenthesis are standard errors of medians.

[4]For each adult survival time, 7 models were fitted; (i) λ and $ln(\delta)$ only (intercept only), (ii) λ_i for each temperature without separating between males and females, (iii) λ_i for each batch (i.e. replication in time for each temperature) without separating between males and females, (iv) λ_i for each temperature and an additive factor λ_{sexm} for the difference between males and females, (v) λ_i for each batch and an additive factor λ_{sexm} for the difference between males and females, (vi) each sex in each temperature and (vii) λ_i for each sex in each batch. Each higher level model reduced the deviance significantly ($P < 0.05$); however, AICc revealed model 5 being the best. Medians present here are from model 6, while λ_{sexm} and $ln(\delta)$ are the results from model 5.

[5]For oviposition time, 3 models were fitted; (i) λ and $ln(\delta)$ only (intercept only), (ii) λ_i for each temperature and (iii) λ_i for each batch (i.e. replication in time for each temperature). Each higher level model reduced the deviance significantly ($P < 0.05$); however, AIC_c revealed model 3 being the best. Medians present here are from model 2, while $ln(\delta)$ resulted from model 3.

Adult lifespan and fecundity

The longevity of adults as well as the time span until females oviposited 50% of their eggs (henceforth referred to as median oviposition time) decreased significantly with increasing temperature. Variation among individuals within cohorts across all temperatures (fixed variance) was in both, survival times and median oviposition times, best described with a Weibull link function (table 4). The models were fitted at different levels of complexity – that is, for the adult live time, the model was fitted with (i) individual parameters to each temperature (batches exposed to the same temperature were pooled) and then (ii) to each of the batches; in addition, (iii) individual parameters were estimated for males and females or (iv) using a single additive factor for males. The lowest AIC_c was obtained when parameters were fitted to each batch (replications in time) with the use of an additive parameter, λ_{sexm}, which estimates the difference in the survival time of males compared with females across all temperatures. The lifetime of males was on average 4.3% [i.e. $1-\exp(\lambda_{sexm})$] shorter than female's (table 4). Temperature-dependent adult median senescence time in adults as well as median oviposition times could be significantly described by linear functions (see fig. 3a,b, table 5) (due to increasing variances with increasing medians the function was fitted in terms of *ln* times). The AIC_c values indicated that the function using generally 4.3% reduced survival time for males (while intercept and slope were set global for males and females) was most likely the best model for describing both male and female longevity. Median oviposition time could be significantly described by the same model; however, fitting the function with individual parameters

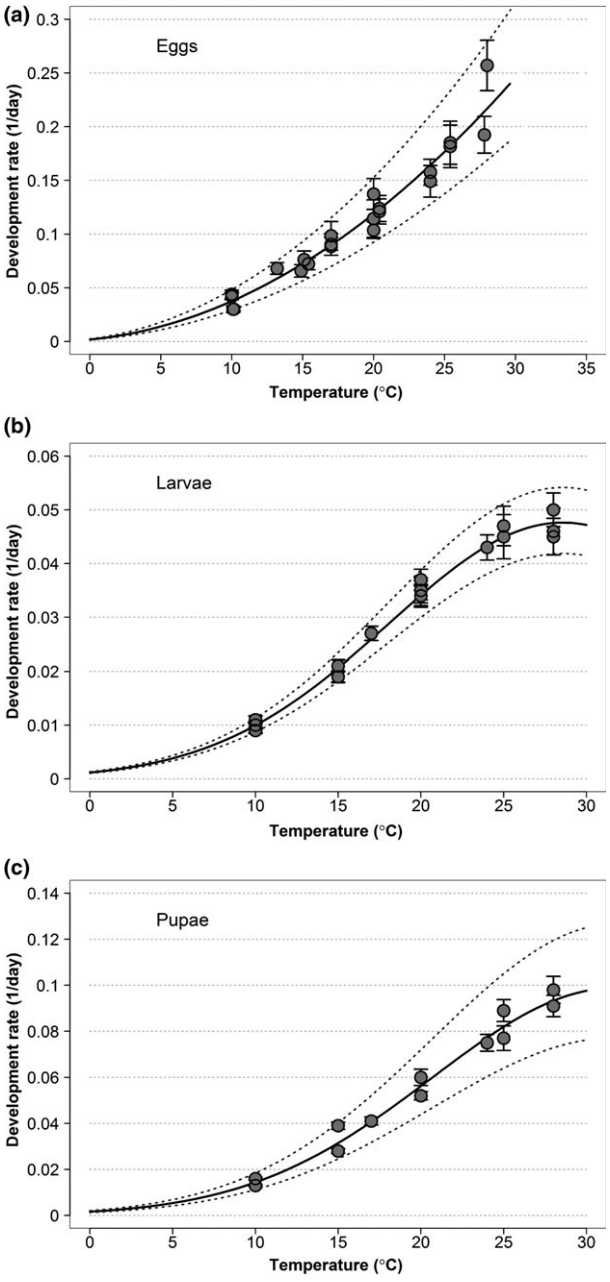

Fig. 1 The relationship between temperature and median development rates for immature life stages of *S. tangolias* (a: eggs, b: larvae, c: pupae). The models, in a: square root model of Ratkowsky et al. (1982), in b and c: Taylor model (Pradhan 1945; Taylor 1981), were fitted in terms of *ln* development time instead of development rate. Broken lines represent 95% confidence limits for the fitted model. Markers are observed median development rates (batches). Bars represent 95% confidence limits of observed data points.

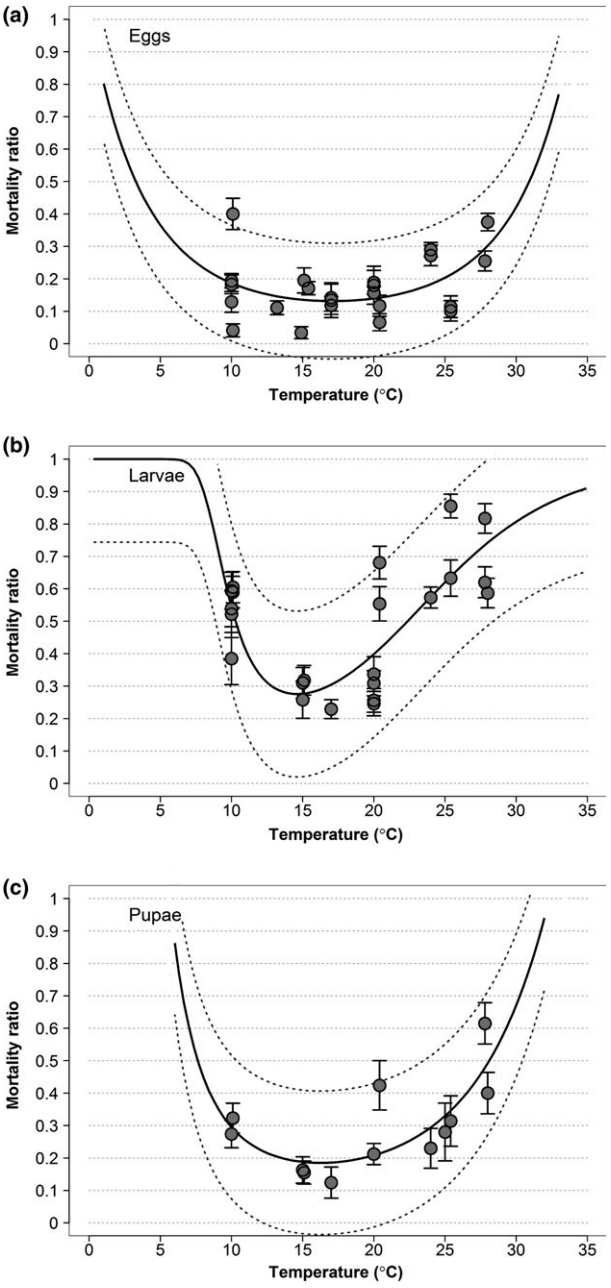

Fig. 2 Temperature-dependent mortality ratios of *S. tangolias* immature life stages (markers: observed mortality rates in each replicate [batch]). Lines: Nonlinear models fitted; broken lines: upper and lower 95% confidence limits of the model. Bars represent 95% confidence limits of observed data points.

revealed 6.8 times higher probability (AIC's evidence ratio) than the model using simply an additive factor relating median oviposition time to median female survival time. Therefore, there is a strong linear relationship between the *ln* median female senescence time and the *ln* median oviposition time, but the ratio between the two figures is not constant across temperatures. At cooler temperatures, females had a relatively more prolonged post-oviposition period than oviposition period (i.e. 50% of the eggs were laid

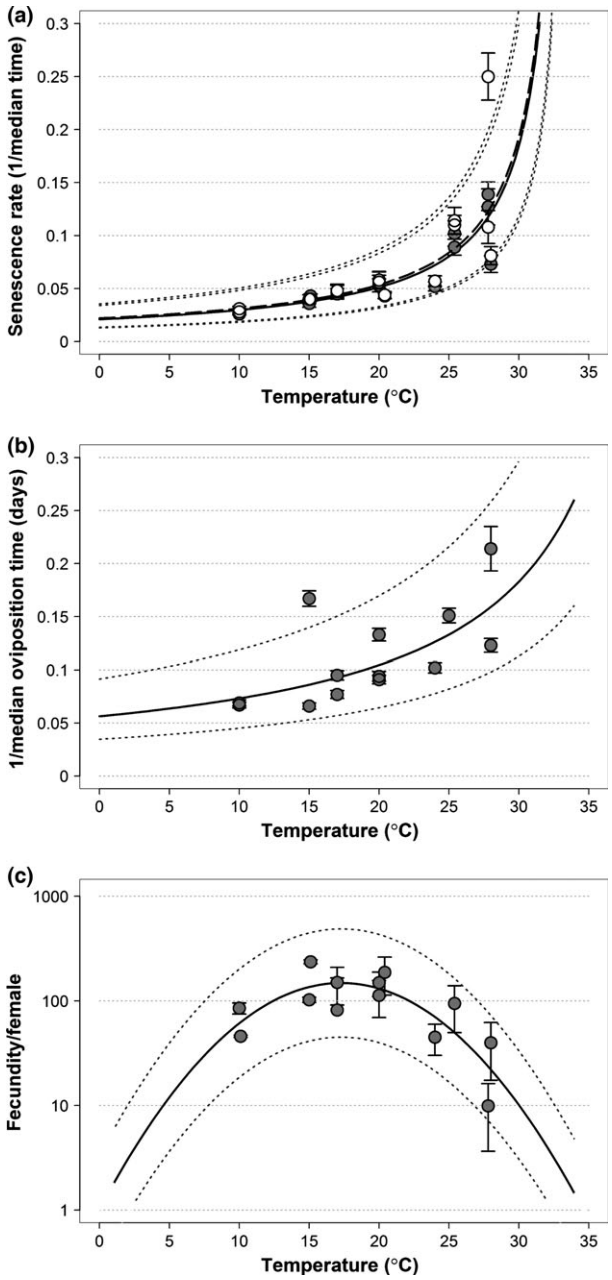

Fig. 3 Temperature-dependent senescence rates (day^{-1}) for *S. tangolias* adults (a), median oviposition time (b) and total fecundity per female. Dots are observed data (in a open dots are males); solid lines are fitted curves (in a+b: exponential model, in a: males lived 4.4% shorter than females – bold broken line), in (c): second-order polynomial model), broken lines: 95% confidence limits for the fitted model (for parameters and statistical regression results, see table 5). Bars represent standard deviation in observed data.

when females terminated about 40% of their live time). Instead, at warmer temperatures, females' relative post-oviposition period decreased rapidly with increasing temperature. At about 30°C, medium oviposition time almost corresponded with the female median lifetime. Thus, age-related oviposition frequencies were better described by the function established for temperature-dependent 'median oviposition time'.

Temperature-dependent total fecundity per female could be described by a quadratic function in which fecundity decreased symmetrically from a maximum of 148 eggs per female at a temperature of 17.3°C (fig. 3c, table 5). Some asymmetric models fitted equally or better to the data (the symmetric function revealed a $\Delta AIC_c = 0.11$, evidence ratios <1.1 compared to the best function); however, the data did not support selecting a model that could reliably predict the minimum and maximum temperature thresholds for fecundity.

For simulating the temperature-dependent age-specific reproduction, female age was normalized using the expected temperature-dependent median oviposition time. The Weibull function predicted best the age-specific oviposition relative frequencies (fig. 4). In the final oviposition model, the difference in the relative frequencies between the time intervals t_{x-1} and t_x (Δtime) was multiplied with the expected temperature-dependent total fecundity to predict age-specific, temperature-dependent reproduction in *S. tangolias* in a given time increment. Figure 4 shows how these simulated reproduction frequencies correspond with the observed data.

Validation of the model

For most of the generation cycles, simulations predicted well the development time and mortality of immature life stages when compared with observed data collected by Keller (2003) (table 6). In general, egg development was quite exactly simulated. In some cycles, the differences between simulated and observed egg development times were significant – on average, simulated development time was about 21% shorter than observed. Development time from egg to pupa and from egg to adult, however, showed good predictions, even if some particular differences were significant. On average, development time from egg to pupa was 3% underestimated by the model, while overall development time from egg to adult was 6% overestimated. Highest discrepancy in overall development time was observed in cycle 4 (+20.4%, see table 6). Mortality was generally well predicted (most figures did not reveal significant differences between observations and simulations); however, on average, overall simulated immature mortality was about 24.4% lower than observed by Keller (2003). As mor-

Table 5 Models and their parameters fitted to describe temperature-dependent senescence rates in adults, median oviposition time and total fecundity per female in *Symmetrischema tangolias*

Life stages	Model[2]		Parameters[1]	F-value	$df_{1,2}$	P	adj. R^2
Adult senescence rate	Simple exponential	b_1	47.66 (±4.05)***	123	1, 28	>0.001	0.8084
		b_2	−1.408 (±0.15)***				
		sex_m	−0.0441 (fixed)				
Median oviposition time^{-1}	Simple exponential	b_1	17.75 (±0.1656)***	10.19	1, 11	0.009	0.4336
		b_2	−0.4096 (±0.0038)***				
Total fecundity per female	Quadratic	T_{opt}	17.3 (±0.93)***	19.4	2, 10	>0.001	0.66
	$ln\ f(T) = r_{max} + c(T_{opt}-T)^2$	r_{max}	4.999 (±0.205)***				
		c	−0.0166 (±0.0045)**				

[1]Numbers in parenthesis are standard errors. Parameter values significantly different from zero are indicated by asterisks (P < 0.05 = *, P < 0.01 = **, P < 0.001 = ***).

[2]Adult senescence rate (simple exponential): if female $r(T) = 1/(b_1 + b_2\,T)$, if male $r(T) = 1/(b_1 + b_2\,T) \times \exp(sex_m)$, Median oviposition time^{-1} (simple exponential): $1/D(T) = 1/(b_1 + b_2\,T)$

Total *ln* fecundity per female: $ln\ f(T) = r_{max} + c(T_{opt}-T)^2$; maximum fecundity ($\exp[r_{max}] = 148$) at T_{opt}.

tality is quite variable, and because an overestimation of mortality is inferior than underestimation when predicting the pest's growth potential, the current models seem suitable for predicting the pest's growth potential.

Life table parameters

At constant temperatures, predicted life table parameters show that *S. tangolias* develops within temperature ranges of about 8–28.8°C (fig. 5). Maximum population growth occurs at around 21°C with a finite rate of increase, λ, of 1.053. However, at fluctuating temperatures, the temperature curves of the life table parameters change as explained by the Kaufmann effect. We simulated temperatures with ±5°C daily fluctuations. To be precise, these simulations were carried out in hourly intervals using a sine wave function between the daily minimum temperature (average temperature minus 5°C) and maximum temperature (average temperature plus 5°C). The results, visualized as a grey line in fig. 5, illustrate the Kaufmann effect. As expected, the temperature–life table parameter curves flatten, with population development thresholds at minimum mean temperature of 6°C (±5°) and maximum mean temperature of 29.5°C (±5°). Accordingly, the mean temperature for maximum population growth raised to around 21.5°C (±5°) with a finite rate of increase, λ, of 1.05.

Discussion

Symmetrischema tangolias has been described as the most cold-tolerant species of the potato tuber moth complex. The species dominates in higher altitudes, particularly >3000 m asl – indeed, it is often the only species – whereas *P. operculella* and *T. solanivora* are more abundant at lower altitudes in the Andean region (Keller 2003; Dangles et al. 2008). Keller (2003) compared development times of *S. tangolias* and *P. operculella* in different locations over an 18-month period at ambient temperatures (by estimating the number of generations per year), but his results do not provide other population growth parameters. Dangles et al. (2008) determined development time, survival and fecundity of all three species at constant temperatures of 10°C, 15°C and 20°C and compared the species physiological performance with the species distribution observed in a variety of environments in Ecuador. The authors found that the best predictor of field abundance was temperature combined with a species × temperature interaction term. In subsequent research, Dangles et al. (2009, 2012) studied the interaction among the three species and showed that the coexistence of the species caused more damage than one pest alone at the same moth density, and proposed a conceptual model that views interaction along a thermal stress depending on species thermal optima. The authors highlighted the importance of knowing nonlinear effects of temperature on process rates in predicting the pests' growth performances.

In the present study, we investigated the temperature dependence of all physiological processes of *S. tangolias* over the full range of temperatures in which the species is expected to develop. Developed functions were used to predict temperature-dependent life table parameters (e.g. finite rate of increase, λ). Minimum and maximum temperature thresholds for population development were determined as 8°C

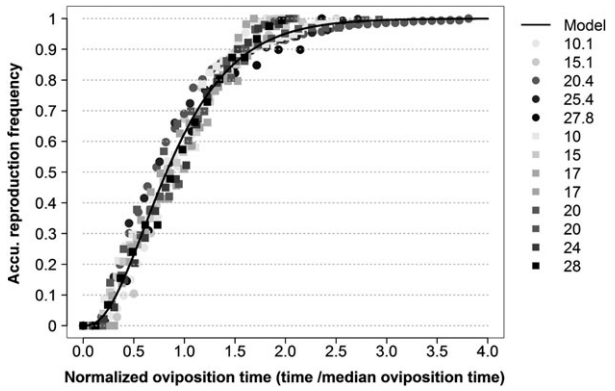

Fig. 4 Cumulative proportion of egg production in relation to female age expressed as normalized time (oviposition time/mean oviposition time). Symbols are observed data (accumulated mean reproduction/total reproduction per female) at indicated experimental temperatures; the line is the Weibull distribution model fitted to the data.

and 28.8°C (fig. 5), with a maximum population growth at 21°C (λ = 1.053). The modelling results on development times, survival and reproduction capacity are in line with the results obtained under the constant temperature experiments conducted by Dangles et al. (2009). In addition, the model performed acceptably well when compared to life table data obtained by Keller (2003) under natural fluctuating temperature conditions. In the present study, the physiological processes were also evaluated at temperature >20°C, which to our knowledge have not been studied before. Dangles et al. (2008, 2009, 2012) contributed to a better understanding of the intraspecies interaction, species distribution and damage potential of the three potato tuber moth species in the Andean region. The present work, however, provides a process-based physiological model that can be applied at any environment (location) and so enable the population growth parameters (life table parameters) to be estimated globally based on temperature. The established models are valid for the two populations of different origin studied. A comparison of the newly established phenology model for *S. tangolias* with the previously established phenology model for *P. operculella* (Sporleder et al. 2004) shows that the growth potential of *S. tangolias* is lower than that of *P. operculella* at temperatures >15°C, whereas at temperatures <15°C, *S. tangolias* has a higher growth potential than *P. operculella* (fig. 6). This might be the reason why *S. tangolias* did not spread out globally across

Table 6 Observed (after Keller 2003) and simulated development times and mortalities in *S. tangolias* eggs, larvae and pupae of six different cohort experiments (generation cycles developed per year at Huancayo, 3350 m asl)

Cycle		Temperature		Egg to Larva		Egg to Pupa		Egg to Adult	
No.	Date (d-m-y)	Min (°C)	Max (°C)	dev. time (days)	Mortality (%)	dev. time (days)	Mortality (%)	dev. time (days)	Mortality (%)
1	01–09–98	5.6	20.5	18.3 (0.81)	25.7 (8.56)	78.8 (2.85)	69.3 (9.04)	102.9 (3.33)	81.3 (7.64)
				18 [−0.41]	28.9 [0.38]	70 [−3.09]	57.2 [−1.35]	105 [0.65]	62.4 [−2.48]
				P = 0.685	P = 0.708	P = 0.002**	P = 0.179	P = 0.519	P = 0.013*
2	11–12–98	6.9	18.2	17.6 (0.9)	21.7 (8.07)	77.2 (3.15)	76.3 (8.33)	105.2 (3.77)	87.3 (6.52)
				17 [−0.7]	17.6 [−0.5]	75 [−0.7]	52.8 [−2.83]	116 [2.86]	58.7 [−4.4]
				P = 0.486	P = 0.615	P = 0.484	P = 0.005**	P = 0.004**	P < 0.001***
3	27–03–99	1.6	19.5	20 (0.78)	25.3 (8.52)	87.1 (5.66)	75.7 (8.41)	133.5 (3.96)	87.7 (6.44)
				18 [−2.62]	19.2 [−0.73]	87 [−0.02]	60 [−1.87]	135 [0.37]	67.3 [−3.16]
				P = 0.009**	P = 0.468	P = 0.984	P = 0.062	P = 0.713	P = 0.002**
4	13–09–99	5.6	20.1	19.7 (1.24)	10.7 (6.05)	67.8 (2.41)	43.7 (9.72)	95.5 (3.2)	63.3 (9.45)
				18 [−1.35]	21.4 [1.78]	78 [4.22]	57.2 [1.39]	120 [7.64]	63.5 [0.02]
				P = 0.175	P = 0.075	P < 0.001***	P = 0.163	P < 0.001***	P = 0.985
5	16–12–99	6.0	18.0	21.2 (1.16)	9.3 (5.7)	80.8 (2.2)	65 (9.35)	122.3 (5.73)	80.7 (7.74)
				17 [−3.59]	19.6 [1.8]	80 [−0.36]	52.2 [−1.37]	127 [0.82]	58.5 [−2.86]
				P < 0.001***	P = 0.072	P = 0.719	P = 0.172	P = 0.411	P = 0.004**
6	16–04–00	2.2	19.8	33.7 (1.16)	16.3 (7.25)	96.1 (5.55)	45.7 (9.76)	131.5 (12.7)	65.7 (9.31)
				19 [−12.61]	23.9 [1.04]	84 [−2.18]	59.9 [1.45]	130 [−0.12]	66.1 [0.04]
				P < 0.001***	P = 0.296	P = 0.029*	P = 0.146	P = 0.905	P = 0.965

Numbers in parentheses are standard deviations calculated from three observed life tables (initial n = 300) and four simulations (n = 100).
For each cycle, the figures above are results from Kellers's observed data (mean of 3 repetitions with n = 100) and the figures below are results from simulations; number in [] is the *z*-value calculated *z* = (simulated value − observed value)/observed STD. P-values revealing significant differences between simulated and observed results are indicated by asterisk (P < 0.05 = *, P < 0.01 = **, P < 0.001 = ***).

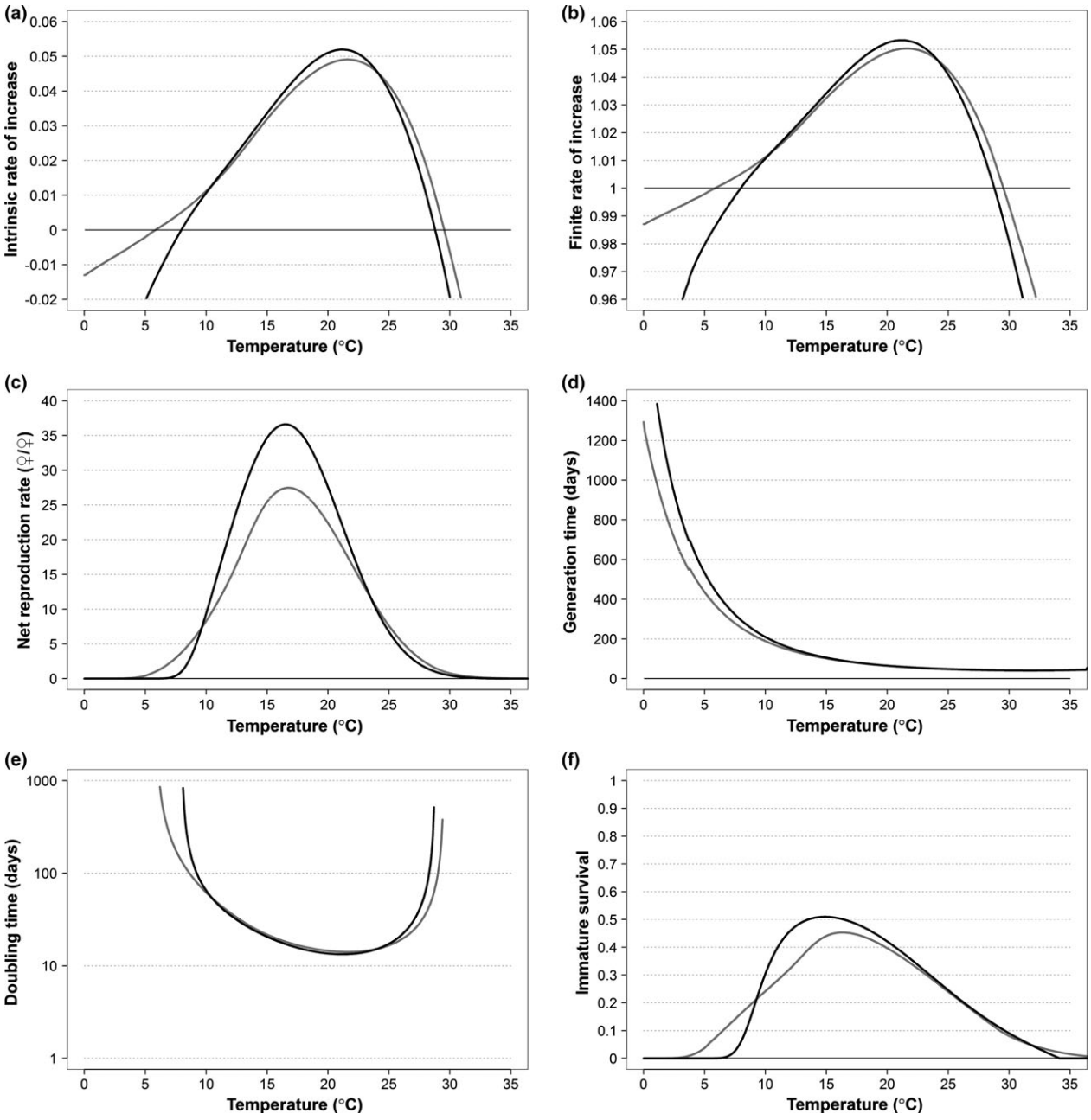

Fig. 5 Life table parameters of *S. tangolias* simulated using the phenology model developed in this study over a temperature range of 0–35°C. (a) Intrinsic rate of natural increase (r_m), (b) finite rate of increase (λ), (c) net reproduction rate (R_0) (females/female), (d) mean generation time (T) (days), (e) doubling time (Dt) (days) and (f) immature survival rate. Black line: simulation result if temperature is hold constant; grey line: simulation result if temperature fluctuates ±5°C (x-value ±5°C).

tropical and subtropical potato production zones, where temperatures regularly exceed 15°C, as *P. operculella*.

As a further advantage, the established model can be applied using daily fluctuating (or even seasonally oscillating) temperatures coping well with the Kaufmann effect (Worner 1992). That is, the temperature–growth performance curve flattens with increasing temperature fluctuations when plotted against mean temperatures, thereby indicating that development is also possible at mean temperatures outside the determined temperature limits (as

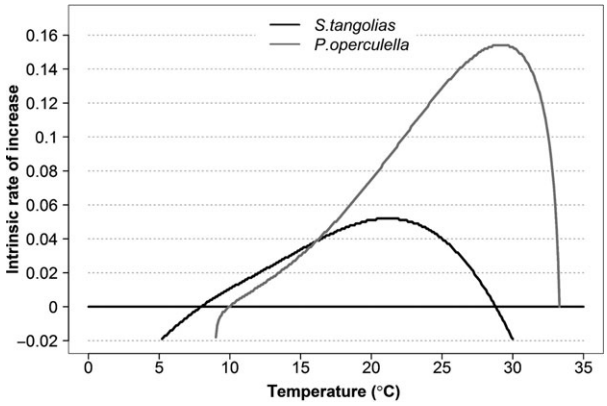

Fig. 6 Comparing the population growth potential between *S. tangolias* and *P. operculella* at constant temperature. The intrinsic rate of increase for *P. operculella* was simulated using the model of Sporleder et al. (2004). The prediction indicates that *P. operculella* has a much higher population increase rate than *S. tangolias*; however, <15°C *S. tangolias* populations are expected to grow faster than *P. operculella*.

demonstrated in fig. 5). This illustrates that the pest might also develop at locations or during seasons in which the mean temperature is below the determined temperature limit. The approach also allows determining the variances expected in individual development processes. For example, variances in development times can be split in the variance that occurs among individuals in a given group of insects of the same age exposed to the same temperature; we called this fixed variance according to Yurk and Powell (2010) and the variance that occurs among different groups or populations at a given temperature (variable variance). In our study, the variance in a given group of insects tested (batches) could be significantly described using a distribution function with a common scale parameter across all temperatures. This confirms the one-shape theory proposed by Curry et al. (1978) that refers to the overlapping of the distributions at different temperature when the insects' age is properly normed. This allows introducing stochastic components in individual physiological processes and simulating life tables with its expected variances (stochastic simulation).

The established model produces reasonable life table parameters for the pest based on temperature and is therefore applicable on a global scale; however, some limitations exist. Survivorship and fecundity are important parameters influencing the final population growth; yet, these parameters are remarkably more variable than the development time in immature life stages. And although the two investigated *S. tangolias* populations revealed certain differences in their survival and reproduction pattern, common functions could be fitted to these parameters. Albeit our submodels for mortality and total female fecundity were supported statistically, the sample did not support a definite assessment of the mortality and fecundity curve at extreme low and high temperatures. Further, additional life table data derived from temperatures <10°C and >28°C would be helpful to improve the model. Keller (2003) pointed out that the phenology of *S. tangolias* in the Mantaro Valley in Peru cannot be explained by means of temperature alone. He could not find an overwintering field population and observed that larvae failed to develop in tubers exposed to direct sunlight. Instead, monitoring the flight activity of *S. tangolias* during four consecutive years from 2011 to 2014 revealed a year-round activity at altitudes of 3214–4010 m asl but with very low numbers during winter months (J. Kroschel, pers. observation). Particularly for year-round simulation of life table parameters, it would be important to assess well the survival pattern at extreme temperatures. Overwintering niches are always important to consider for any pest that might support re-infestation of fields. It also remains to link the simulated life table parameters with the feeding performance and damage potential and hence the economic impact of the pest species at a given environment.

Conclusion

Our study assessed the temperature-dependent development of *S. tangolias* and developed a temperature-driven phenology model for this potato pest, which is essential knowledge for setting up local pest management programmes, or analysing the pests' establishing risks and potential abundance under current and future climates. In future research, the model will be used to project the establishment risk of *S. tangolias* based on long-term interpolated temperature data (WorldClim) in a geographic information system (GIS) environment and possible distribution changes due to climate change using the ILCYM software. Future research will also address the implementation of stochastic components to simulate the growth potential with reliable realistic errors and how the knowledge on species interaction among the three potato tuber moth species can be used to sophisticate the model outputs.

Acknowledgements

This work was funded by the Federal Ministry of Co-operation and Development (BMZ), Germany. We thank Patricio Gallegos for hosting Birgit Schaub at the National Institute for Agricultural Research (INIAP), Ecuador, and his support for conducting the life table experiments in Ecuador. Further, we acknowledge receipt of the financial support to Birgit Schaub from the German Academic Exchange Service (DAAD).

References

Akaike H, 1973. Information theory as an extension of the maximum likelihood principle. In: Second International Symposium on Information Theory. Ed. by Petrov BN, Csaki F, Akademiai Kiado, Budapest, 276–281.

Andrewartha HG, Birch C, 1954. The distribution and abundance of animals. University of Chicago Press, Chicago.

Bale JS, Masters GJ, Hodkinson ID, Awmack C, Bezemer TM, Brown VK, Butterfield J, Buse A, Coulson JC, Farrar J, Good John E G, Harrington R, Hartley S, Jones TH, Lindroth RL, Press MC, Symrnioudis I, Watt AD, Whittaker JB, 2002. Herbivory in global climate change research: direct effects of rising temperature on insect herbivores. Global Change Biol 8, 1–16.

Campbell A, Frazer BD, Gilbert N, Gutierrez AP, MacKauer M, 1974. Temperature requirements of some aphids and their parasitoides. J App Ecol 11, 431–438.

Curry GL, Feldman RM, Sharpe PJH, 1978. Foundations of stochastic development. J Theor Biol 74, 397–410.

Dangles O, Carpio C, Barragan AR, Zeddam JL, Silvain JF, 2008. Temperature as a key driver of ecological sorting among invasive pest species in the tropical Andes. Ecol Appl 18, 1795–1809.

Dangles O, Mesías V, Crespo-Perez V, Silvain J, 2009. Crop damage increases with pest species diversity: evidence from potato tuber moths in the tropical Andes. J Appl Ecol 46, 1115–1121.

Dangles O, Herrera M, Mazoyer C, Silvain J, 2012. Temperature-dependent shifts in herbivore performance and interactions drive nonlinear changes in crop damages. Global Change Biol 19, 1056–1063.

Dangles O, Herrera M, Anthelme F, 2013. Experimental support of the stress-gradient hypothesis in herbivore-herbivore interactions. New Phytol 197, 405–408.

Hurvich CM, Tsai CL, 1989. Regression and time series model selection in small samples. Biometrika 76, 297–307.

Keller S, 2003. Integrated pest management of the potato tuber moth in cropping systems of different agro-ecological zones. Ed. by Kroschel J. Advances in Crop Research, vol 1. Margraf Verlag, Weikersheim, Germany. 163p.

Kroschel J, Schaub B, 2013. Biology and Ecology of Potato Tuber Moths as Major Pests of Potato. In: Insect pests of potato. Global perspectives on biology and management. Ed. by Alyokhin A, Vincent C, Giordanengo P, Elsevier, London, Waltham, MA, 165–192.

Kroschel J, Sporleder M, Tonnang HEZ, Juarez H, Carhuapoma P, Gonzales JC, Simon R, 2013. Predicting climate-change-caused changes in global temperature on potato tuber moth *Phthorimaea operculella* (Zeller) distribution and abundance using phenology modeling and GIS mapping. Agr Forest Meteorol 170, 228–241.

Logan JA, 1988. Toward an expert system for development of pest simulation models. Environ Entomol 17, 359–376.

Logan J, Wollkind D, Hoyt S, Tanigoshi L, 1976. An analytic model for description of temperature dependent rate phenomena in arthropods. Environ Entomol 5, 1133–1140.

Maia AHN, Luiz AJ, Campanhola C, 2000. Statistical inference on associated fertility life table parameters using jackknife technique: computational aspects. J Econ Entomol 93, 511–518.

Martin NA, 1999. Arthropods and molluscs associated with poroporo (*Solanum aviculare* and *S. laciniatum*). J Roy Soc New Zeal 29, 65–76.

McCornack BP, Ragsdale DW, Venette RC, 2004. Demography of soybean aphids (Homoptera: Aphididae) at summer temperatures. J Econ Entomol 97, 854–861.

Osmelak JA, 1987. The tomato stemborer *Symmetrischema plaesiosema* (Turner), and the potato moth *Phthorimaea operculella* (Zeller), as stemborers of pepino: first Australian record. Plant Prot Q (Aust) 2, 44.

Palacios M, Tenorio J, Vera M, Zevallos FE, Lagnaoui A, 1999. Population dynamics of the Andean potato tuber moth, *Symmetrischema tangolias* (Gyen), in three different agro-ecosystems in Peru. In: Impact on a changing world: program report 1997–1998. Ed. by Arthur C, Ferguson P, Smith B, International Potato Center (CIP), Lima, Peru, 153–160.

Pradhan S, 1945. Insect population studies. II. Rate of insect development under variable temperatures of the field. Proc Natl Inst Sci India 11, 74–80.

R Development Core Team, 2011. R: a language and environment for statistical computation. R Foundation for Statistical Computing, Vienna, Austria.

Ratkowsky DA, Olley J, McMeekin TA, Ball A, 1982. Relationship between temperature and growth rate of bacterial cultures. J Bacteriol 149, 1–5.

Schoolfield R, Sharpe PJH, Magnuson C, 1981. Non-linear regression of biological temperature-dependent rate models based on absolute reaction-rate theory. J Theor Biol 88, 719–731.

Sporleder M, Kroschel J, Quispe Maritza R Gutierrez, Lagnaoui A, 2004. A temperature-based simulation model for

the potato tuberworm, *Phthorimaea operculella* Zeller (Lepidoptera; Gelechiidae). Environ Entomol 33, 477–486.
Sporleder M, Tonnang HEZ, Carhuapoma P, Gonzales JC, Juarez H, Kroschel J, 2013. Insect Life Cycle Modelling (ILCYM) software - a new tool for regional and global insect pest risk assessments under current and future climate change scenarios. In: Potential invasive pests of agricultural crops. Ed. by Peña JE, CABI, Wallingford, 412–427.
Taylor F, 1981. Ecology and evolution of physiological time in insects. Am Nat 117, 1–23.
Tonnang E, Carhuapoma Juarez HP, Gonzales JC, Sporleder M, Simon R, Kroschel J, 2013. ILCYM - Insect Life Cycle Modeling. A software package for developing temperature-based insect phenology models with applications for regional and global analysis of insect population and mapping. ILCYM 3.0 user manual. International Potato Center (CIP), Lima, Peru.
Uvarov BP, 1931. Insects and climate. T Roy Entomol Soc Lon 79, 1–232.
Wagner TL, Wu HI, Sharpe PJH, Schoolfield RM, Coulson RN, 1984. Modeling insect development rates: a literature review and application of a biophysical model. Ann Entomol Soc Am 77, 208–225.
Worner SP, 1992. Performance of phenological models under variable temperature regimes: consequences of the Kaufmann or rate summation effect. Environ Entomol 21, 689–699.
Yurk BP, Powell JA, 2010. Modeling the effects of developmental variation on insect phenology. B Math Biol 72, 1334–1360.
Zamani AA, Talebi AA, Fathipour Y, Baniameri V, 2006. Effect of temperature on biology and population growth parameters of *Aphis gossypii* Glover (Hom., Aphididae) on greenhouse cucumber. J Appl Entomol 130, 453–460.

Supporting Information

Additional Supporting Information may be found in the online version of this article:

Appendix S1. Egg stage: location, temperature, batch numbers, and numbers of individuals evaluated per batch (replication reefers to the number of experimental units – paper sections - used).

Appendix S2. Larval stage: location, temperature, batch numbers, and numbers of individuals evaluated per batch (replication reefers to the number of experimental units – rearing boxes [about 50 larvae were reared together in one box] - used).

Appendix S3. Pupal stage: location, temperature, batch numbers, and numbers of individuals evaluated per batch (replication reefers to the number of experimental units – pupae collected from the same rearing box - used)

Appendix S4. Adult senescence and reproduction: location, temperature, batch numbers, and numbers of individuals (females and males) evaluated per batch (replication reefers to the number of experimental units – cylinders - used). Note that in Ecuador survival was not evaluated from the same individuals as used for evaluating reproduction. For assessing the sub-models for the oviposition model only the data from individuals to assess reproduction were used.

Data S1. EGG development time.

Data S2. LARVA development time.

Data S3. Pupae development time.

Data S4. Adult survival time.

Data S5. Oviposition time.